

Supplementary Information

Macroporous Three-Dimensional MXene Architectures for Highly Efficient Solar Steam Generation

Xing Zhao, Xiang-Jun Zha, Jun-Hong Pu, Lu Bai, Rui-Ying Bao, Zheng-Ying Liu, Ming-Bo Yang,

Wei Yang*

College of Polymer Science and Engineering, Sichuan University, State Key Laboratory of Polymer
Materials Engineering, Chengdu, 610065, Sichuan, China

SI-1 Consumption analysis of solar energy

The energy consumption of the system mainly originates from: (1) the water evaporation, (2) the reflection energy loss, (3) the conduction heat loss from the absorber to the underlying water, (4) the radiation and (5) the convection heat loss from the surface of absorber to the environment.

(1) Water evaporation energy consumption Q_{eva}

According to our evaporation experiment results, the water evaporation energy consumption is 88.7% of all the irradiation energy.

(2) Reflection energy loss Q_{ref}

The measured average reflection rate of the 3DMA over the broad solar spectrum (300 – 1500 nm) is 2%.

(3) Conduction heat loss Q_{cond}

The heat flux of the conduction Q_{cond} can be calculated by: $Q_{\text{cond}} = Cm\Delta T$, where C is the specific heat capacity of pure water ($4.2 \text{ kJ kg}^{-1} \text{ }^{\circ}\text{C}^{-1}$), m denotes the weights of water (50 g), and ΔT ($0.4 \text{ }^{\circ}\text{C}$) represents the average elevated temperature of the underlying water after 1 h solar illumination. Under 1 kW m^{-2} solar irradiation, we can calculate the

*Corresponding author. Tel.: + 86 28 8546 0130; fax: + 86 28 8546 0130.

E-mail addresses: weiyang@scu.edu.cn (W Yang)

conduction heat loss value of 3.3% of all the irradiation energy.

(4) Radiation heat loss Q_{rad}

The heat flux of radiation Q_{rad} is based on the Stefan-Boltzmann law, which can be calculated by: $Q_{\text{rad}} = \varepsilon A \sigma (T_{\text{sur}}^4 - T_{\text{env}}^4)$, where ε is the emissivity (It is assumed that the absorber has a maximum emissivity of 0.9), A is the surface area of absorber under the solar illumination (7.07 cm^2), σ is the Stefan-Boltzmann constant ($5.67 \times 10^{-8} \text{ W m}^{-2} \text{ K}^{-4}$), T_{sur} is the average surface temperature ($\sim 38^\circ \text{C}$) of the absorber at steady state condition, and T_{env} is the ambient temperature ($\sim 33^\circ \text{C}$) upward the absorber under the solar illumination of 1 sun. The radiation heat loss is calculated to be $\sim 3.0\%$ of all the irradiation energy.

(5) Convection heat loss Q_{conv}

The heat flux of radiation Q_{conv} is based on the Newton's law of cooling, which can be calculated by: $Q_{\text{conv}} = hA(T_{\text{mem}} - T_{\text{env}})$, where h is the convection heat transfer coefficient (set as $5 \text{ W m}^{-2} \text{ K}^{-1}$) and A is the surface area (7.07 cm^2) of the 3DMA under solar illumination. Under 1 kW m^{-2} solar irradiation, we can calculate the convection heat loss value of 2.5% of all irradiation energy.

The sum of all the above energy consumption is 99.5%. Excluding test and calculation errors, other pathways of energy consumption loss may also exist.

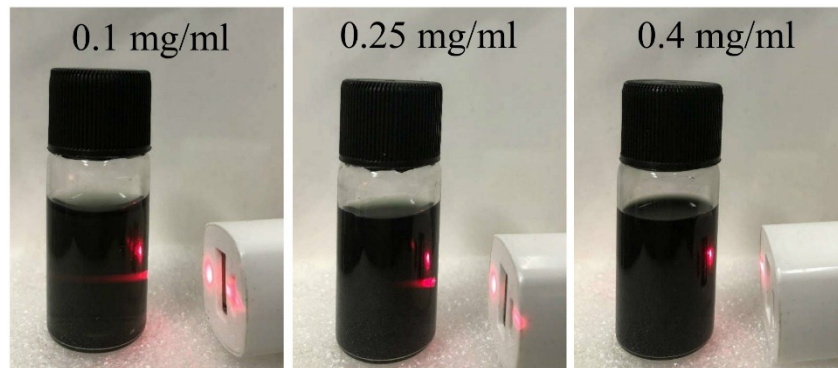


Fig. S1 Tyndall scattering effect in the MXene colloidal suspension with different concentrations. The Tyndall scattering effect in the colloidal suspension with the MXene concentration of 0.1 mg/ml was obvious and the light beam went through the whole glass container, while the beam intensity became weaker with the increase of the MXene concentration.

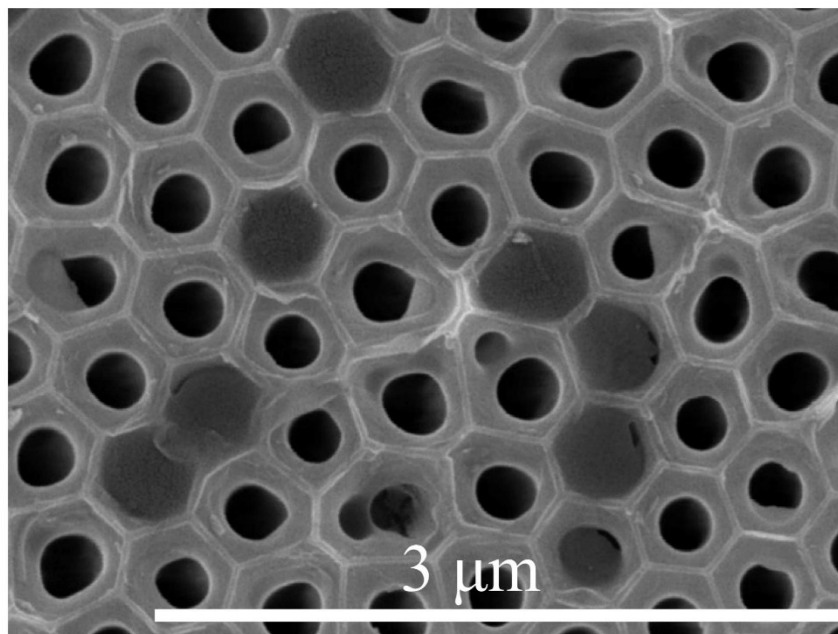


Fig. S2 SEM image of the delaminated MXene nanosheets on porous anodic aluminum oxide (AAO) (scale bar, 3 μm).

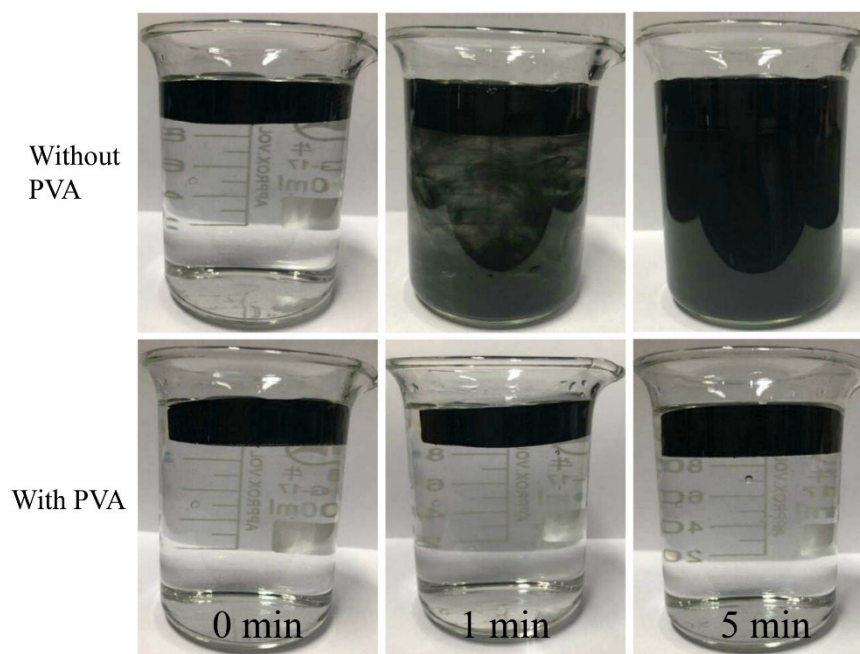


Fig. S3 The photographs of 3DMA without and with PVA after different times of sonication.

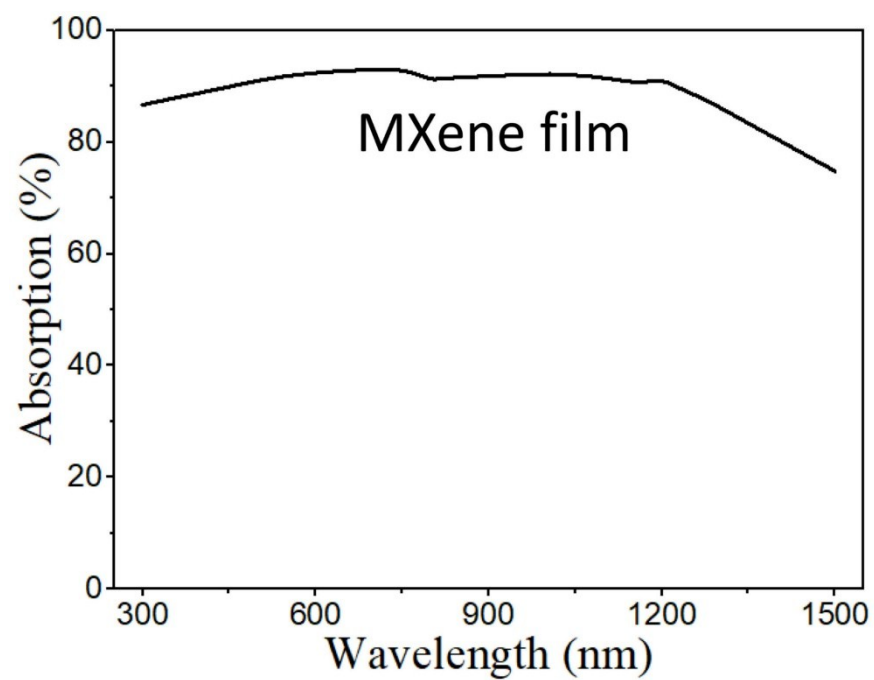


Fig. S4 The light absorption spectra for the MXene film.

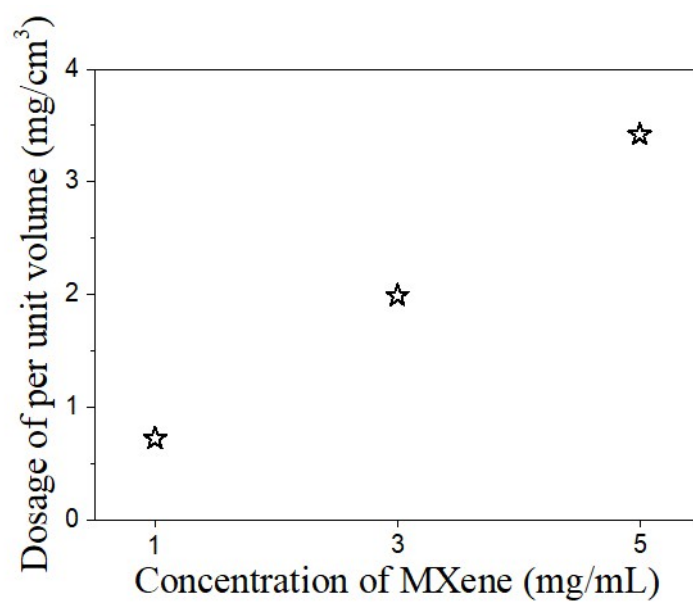


Fig. S5 The actual dosage of MXene per unit volume.

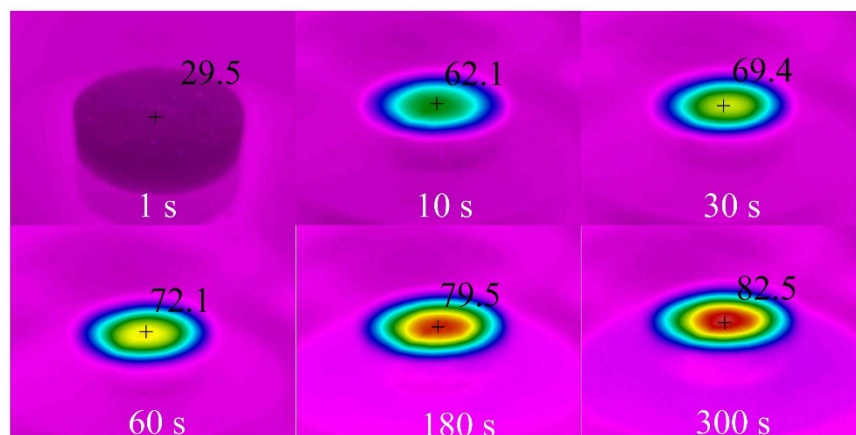


Fig. S6 IR images of 3DMA-5 directly exposed on one sun irradiation for 1, 10, 30, 60, 180 and 300 s.

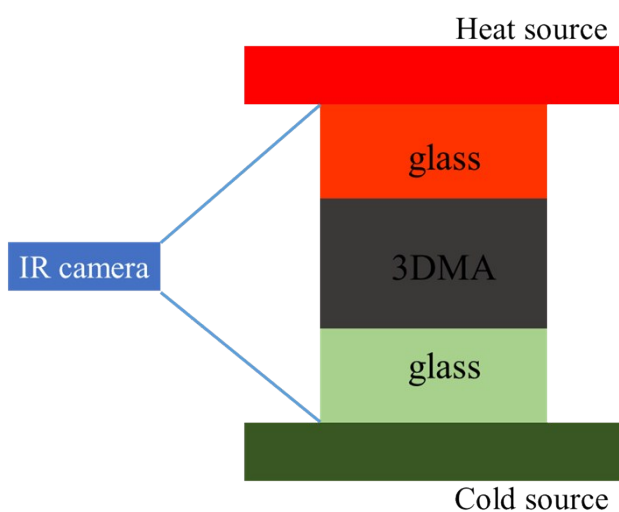


Fig. S7 Schematic illustration of thermal conductivity measurement system

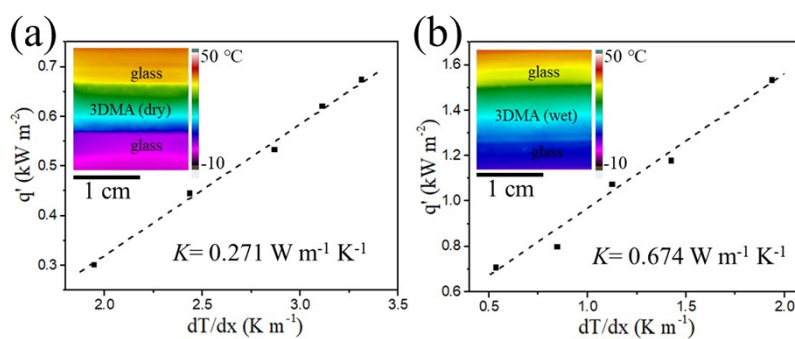


Fig. S8 Thermal conductivity of dry 3DMA (a) and wet 3DMA (b). Insets: Representative IR thermal images showing the temperature distribution along the thickness of the dry/wet 3DMA.

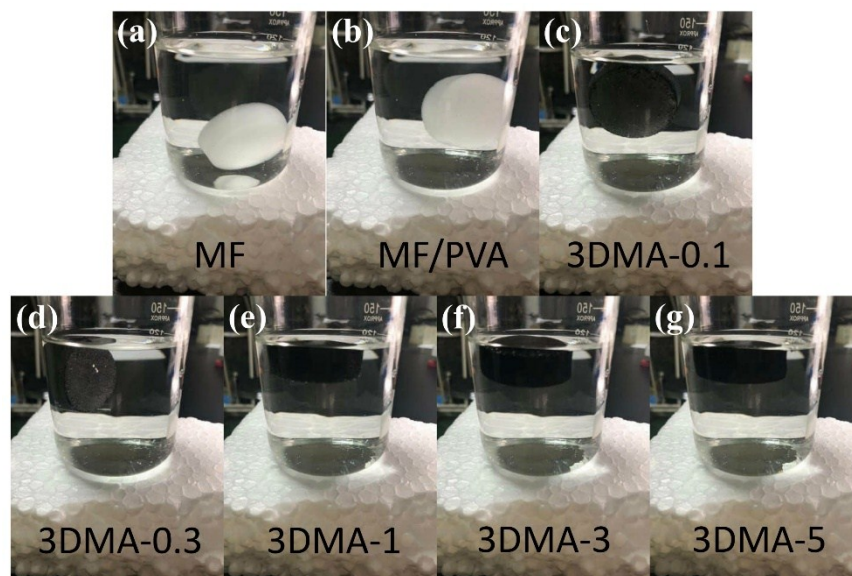


Fig. S9 Optical photos of different samples left in the water after stabilization.

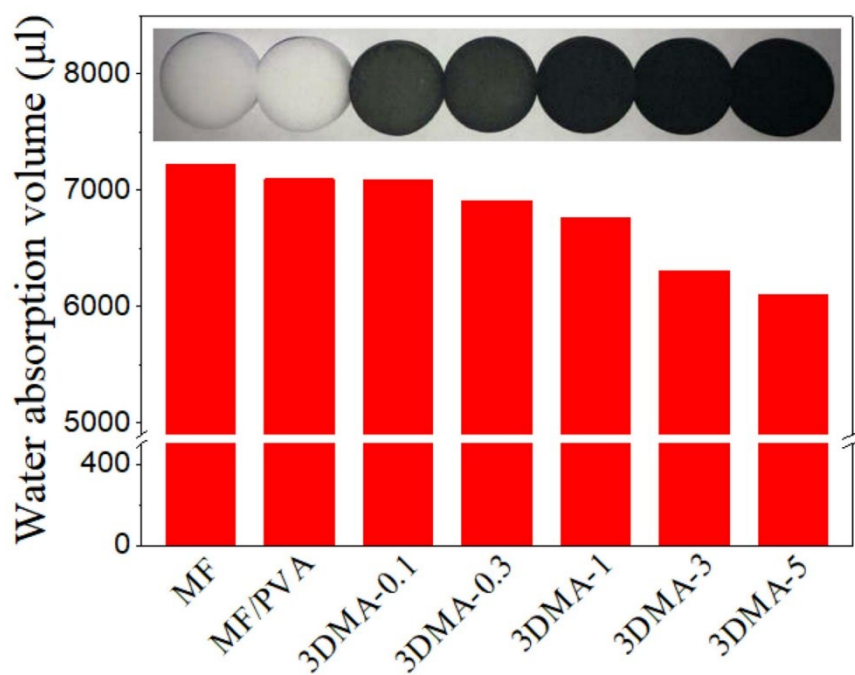


Fig. S10 Water absorption volume of different. Inset is optical photos of samples from MF to 3DMA-5.

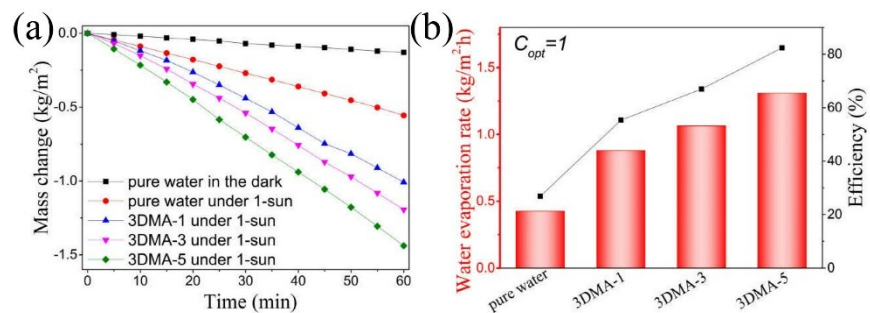


Fig. S11 (a) Mass change of water with different samples under solar illumination of 1 sun. (b) Water evaporation rates (left-hand side axis) and corresponding solar steam efficiency (right-hand side axis) of different system under solar illumination of 1 sun.

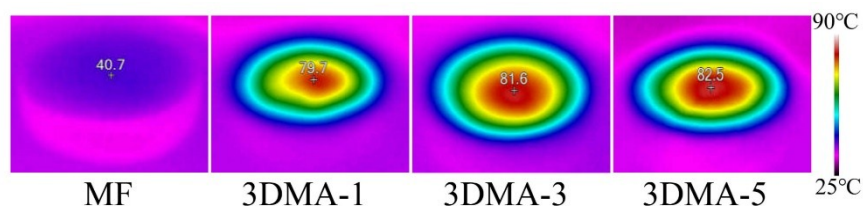


Fig. S12 IR images of MF, 3DMA-1, 3DMA-3 and 3DMA-5 directly exposed on one sun irradiation for 300 s.



Fig. S13 Photographs of both sides of 3DMA with embedded EPE foam.

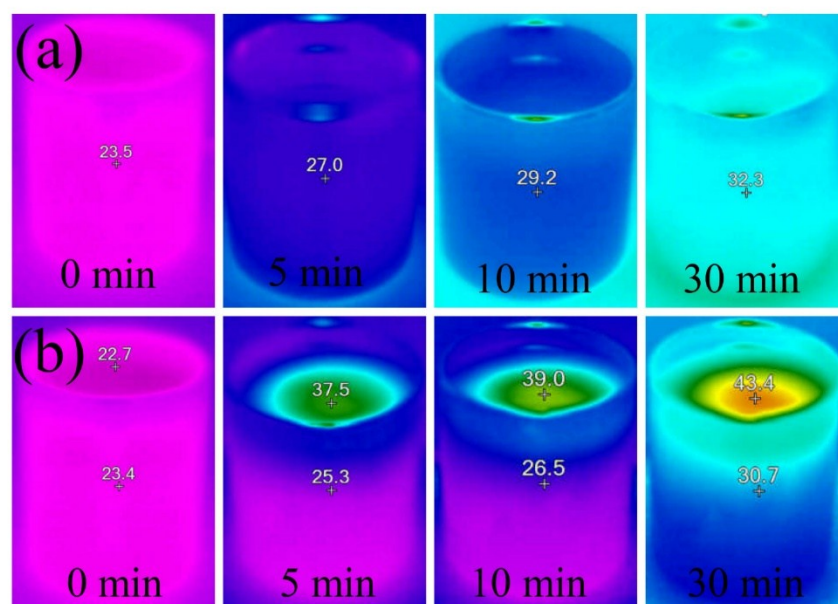


Fig. S14 (a) Temperatures of water without absorbers after 30 min solar illumination of 1 sun. (b) Temperature of water and 3DMA surface without EPE thermally insulating layer.

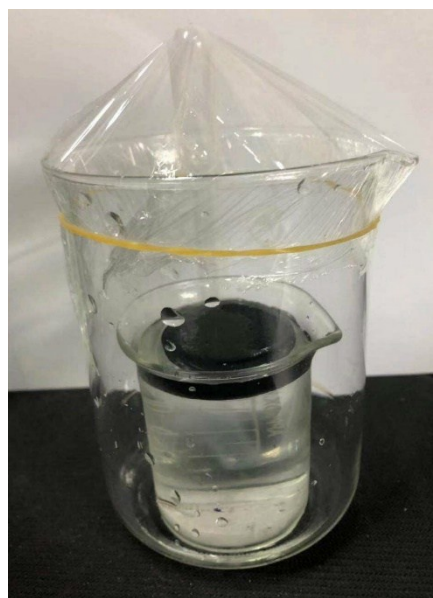


Fig. S15 The photograph of condensed water collecting device.

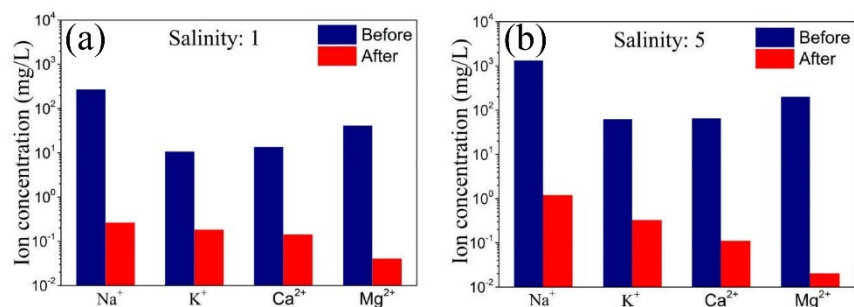


Fig. S16 The measured concentrations of four primary ions in an original seawater sample with salinity of 1 (a) and 5 (b) before (original) and after evaporation.

Table S1 The Smart Quant Results of EDS mapping.

Element	Weight %	Atomic %	Net Int.	Error %	Kratio	Z	R	A	F
C K	36.40	45.04	425.5	5.43	0.23	1.05	0.98	0.60	1.00
N K	33.97	36.05	105.4	10.76	0.05	1.02	0.99	0.15	1.00
O K	13.22	12.28	57.8	11.67	0.01	1.00	1.00	0.09	1.00
F K	3.26	2.55	26.2	12.39	0.00	0.93	1.00	0.13	1.00
TiK	13.16	4.08	422.3	2.28	0.11	0.78	1.08	1.03	1.03

Table S2 Water evaporation rate and solar steam efficiency of different batches of experiments in our work.

sample	Optical concentration	Whether with EPE thermal insulation layer	Evaporation rate (kg/m ² ·h)	efficiency
Pure water	1 sun	no	0.426	26.8
3DMA-1	1 sun	no	0.879	55.3
3DMA-3	1 sun	no	1.064	67.0
3DMA-5	1 sun	no	1.309	82.4
3DMA-5	3 sun	no	3.988	83.7
3DMA-5	5 sun	no	6.997	88.1
3DMA-5	7 sun	no	9.774	87.9
3DMA-5	10 sun	no	13.938	87.7
3DMA-5	1 sun	yes	1.409	88.7
3DMA-5	5 sun	yes	7.486	94.2

Video S1

The water supply of 3DMA in the solar steam generation process. The water immediately reached the surface of the 3DMA and then quickly spread, once the 3DMA was contacted with water.

Video S2

Steam generation under simulated solar illumination of 5 sun.